Published in final edited form as:

AJR Am J Roentgenol. 2014 December ; 203(6): 1345–1352. doi:10.2214/AJR.14.12462.

Imaging Features of Alveolar Soft Part Sarcoma: A Report from Children's Oncology Group Study ARST0332

M. Beth McCarville[1], **Sofia Muzzafar**[1], **Simon C. Kao**[2], **Cheryl Coffin**[3], **David M. Parham**[4], **James Anderson**[5], and **Sheri L. Spunt**[6]

[1]Department of Radiological Sciences, St. Jude Children's Research Hospital, Memphis, TN

[2]Department of Radiology, the University of Iowa Hospitals and Clinics, Iowa City, IA

[3]Department of Pathology, Microbiology and Immunology, Vanderbilt University School of Medicine, Nashville, TN

[4]Department of Pathology and Laboratory Medicine, Children's Hospital of Los Angeles and University of Southern California, Keck School of Medicine, Los Angeles, CA

[5]Department of Biostatistics, University of Nebraska Medical Center, Omaha, NE

[6]Department of Pediatrics, Stanford University School of Medicine, Palo Alto, CA

Abstract

Objective—There is little literature regarding imaging features of alveolar soft-part sarcoma. We performed a comprehensive assessment of imaging characteristics of this rare tumor to determine if there are features that suggest the diagnosis.

Materials and Methods—Twenty-two subjects with alveolar soft-part sarcoma underwent pre-therapy imaging (16 MRIs, 3 CTs, 3 both) as part of enrollment on Children's Oncology Group protocol ARST0332 for treatment of non-rhabdomyosarcoma soft-tissue sarcomas. Two radiologists retrospectively reviewed imaging by consensus and recorded tumor location, size, contour, internal architecture, signal characteristics, presence of flow-voids and enhancement patterns.

Results—The 12 females and 10 males ranged in age from 8 to 23.6 years (mean, 15.7 years). The most common anatomic site was lower extremity (12/22, 55%) followed by upper extremity (4/22, 18%). Maximal tumor diameter ranged from 2.3 cm to 20.0 cm (median, 5.9 cm). All tumors imaged with MRI had flow-voids (19/19, 100%) and 19 (19/22, 86%) had large peripheral

Corresponding author: Beth McCarville St. Jude Children's Research Hospital Department of Radiological Sciences, MS 220 262 Danny Thomas Place Memphis, TN 38105 Beth.mccarville@stjude.org Phone: (901) 595-2399 Fax: (901) 595-3981.
Sofia Muzzafar St. Jude Children's Research Hospital Department of Radiological Sciences, MS 220 332 Danny Thomas Place Memphis, TN 38105 sofiamuzzafar@yahoo.com
Sheri Spunt Stanford University School of Medicine Department of Pediatrics 1000 Welch Road, Suite 300, MC 5798 Palo Alto, CA 94304 sspunt@stanford.edu
Simon Kao The University of Iowa Hospitals and Clinics Iowa City, IA simon-kao@uiowa.edu
Cheryl Coffin Vanderbilt University School of Medicine Department of Pathology, Microbiology and Immunology 1121 21st Avenue South Nashville, TN 37232 ccoffin@hotmail.com
James Anderson University of Nebraska Medical Center College of Public Health 984355 Nebraska Medical Center Omaha, NE 68198-4355 janderson@unmc.edu
David M. Parham, MD Children's Hospital Los Angeles and University of Southern California, Keck School of Medicine Department of Pathology and Laboratory Medicine 4650 Sunset Boulevard, #43 Los Angeles, CA 91100 daparham@chla.usc.edu

vessels, lobulated margins and nodular internal architecture. T1W pre-contrast MR imaging was available for 18 tumors; 14 (14/18, 78%) appeared slightly hyperintense to muscle. Of 16 imaged with contrast, 11 (11/16, 69%) showed intense and 5 (5/16, 31%) moderate enhancement. Six (6/16, 38%) had thick enhancing peripheral rims with non-enhancing centers consistent with necrosis.

Conclusions—Imaging features of alveolar soft part sarcoma include flow voids, large peripheral vessels, internal nodularity and lobulated margins. Contrast administration produces intense to moderate enhancement, sometimes with a thick enhancing peripheral rim around central necrosis. Extremity tumors with these imaging features in a child or young adult should suggest the diagnosis of alveolar soft part sarcoma.

Introduction

Alveolar soft-part sarcoma (ASPS) is a rare solid malignancy that accounts for less than 1% of all soft-tissue sarcomas [1]. It occurs most commonly in adolescents and young adults and has a slight female predominance [2-4]. Typically, ASPS is a slow-growing tumor and often comes to clinical attention late in the disease process. About 65% of adults and 30% of children present with metastatic disease in the lungs, brain, bone and/or lymph nodes. Metastases also occur decades after resection of the primary tumor, even in the absence of local recurrence [2, 5]. The prognosis of patients with ASPS is poor. In a large study by Lieberman and colleagues, survival of 102 subjects dropped from 87% at 2 years to 18% at 20 years [5].

In adults, ASPS has a propensity for the lower extremities but can arise in unusual locations such as the female genital tract, mediastinum, breast, urinary bladder, gastrointestinal tract and bone. In children, ASPS may arise in the head and neck, particularly the orbit and tongue [2, 6-8]. The diagnosis of ASPS relies on histopathology, immunohistochemistry and molecular features. Histologically these tumors have a uniform pattern characterized by a pseudoalveolar or organoid arrangement of polygonal tumor cells separated by fibrovascular septa and delicate capillary-sized vascular channels [9-10]. A characteristic unbalanced translocation, der(17)t(X:17) (p11;q25) results in the formation of an ASPL–TFE3 fusion protein. This translocation is seen almost exclusively in ASPS and some pediatric renal cell carcinomas [10] and rarely in periendothelial epithelioid cell tumors [11]. An antibody directed against the C-terminus of the TEF3 protein is a highly sensitive and specific marker for ASPS. It has been suggested that the increased incidence of ASPS in females is related to their two X chromosomes, which doubles the probability of this translocation as compared to males [10].

The mainstay of treatment for ASPS is complete surgical resection of the primary tumor and radiotherapy for microscopic residual disease at the primary site. In adults, ASPS is known to be resistant to standard chemotherapy. Due to the rarity of this tumor in pediatrics, the role of chemotherapy in this patient population has not been clearly defined. The Children's Oncology Group (COG) recently conducted a large, multi-institutional trial, ARST0332, to investigate a risk-based strategy for treatment of patients under 30 years of age with non-rhabdomyosarcoma soft tissue sarcomas (NRSTS). A total of 551 eligible patients were

enrolled including 25 subjects with ASPS. While there is an abundance of literature regarding the pathological and clinical features of ASPS, there is little published data regarding its imaging features. The ARST0332 study afforded us the opportunity to review the imaging features of ASPS in a relatively large cohort of prospectively enrolled young patients. Therefore, the purpose of this study was to perform a comprehensive review of the imaging features of ASPS and, when possible, to correlate these with the pathological findings. The goal of the study was to improve our understanding of the imaging features of this rare tumor and to identify imaging findings that might suggest the diagnosis to radiologists in their everyday practice.

Material and Methods

The study cohort was comprised of patients under the age of 30 years with ASPS who were enrolled on COG protocol ARST0332 between February 2007 and February 2012. The protocol was HIPAA compliant and IRB approved at the participating institutions; all subjects and/or their guardians signed informed consent or assent as appropriate. The tumors of all patients were centrally reviewed by two expert pediatric soft tissue pathologists (CC, DP) to confirm the histologic subtype of NRSTS. The diagnosis of ASPS was confirmed by the study pathologists based on review of local pathology reports and histologic inspection of biopsy specimens. Additional, supporting immunohistochemical or genenomic testing for ASPS was performed at the discretion of the local institution but was not required for central review. Because we sought to correlate imaging findings with gross pathologic findings of ASPS the study pathologists collected information regarding gross tumor pathology from local pathology reports. Subjects underwent either computed tomography (CT) or magnetic resonance imaging (MRI) of the primary tumor and chest CT and nuclear medicine studies for staging, at their local institution. Imaging was sent prospectively to the Quality Assurance Review Center (QARC) in Lincoln, RI, where patient identifiers were removed and unique identifiers were assigned. The de-identified imaging was reviewed by two central radiologist reviewers (MBM, SK) with 25 and 12 years faculty level experience in pediatric radiology at the beginning of the study period. Both radiologists independently determined tumor measurements in three dimensions and assessed neurovascular and bone involvement. Neurovascular involvement was categorized as, 1) tumor not abutting the neurovascular bundle, 2) tumor abutting the neurovascular bundle or 3) tumor surrounding the neurovascular bundle. Bone involvement was categorized as, 1) tumor not abutting bone, 2) tumor abutting bone or 3) tumor destroying bone. Discrepancies were resolved by consensus between the two study radiologists. The prospectively collected imaging data, as well as demographic and clinical features assessed at study entry, were obtained from the COG database for purposes of the present study.

Imaging review

For purposes of this study the MRI and CT imaging of the ASPS primary tumors, at the time of diagnosis, were re-reviewed by consensus by two radiologists, one of whom was a central reviewer for the ARST0332 study (MBM) and the other a pediatric oncological imaging fellow (SM). Magnetic resonance T1W, T2W, STIR, T1W post contrast, axial, sagittal, and coronal (when available) images were reviewed. From the MR images reviewers determined

the following characteristics: predominant tumor signal intensity relative to muscle (hypointense, isointense or hyperintense), presence of flow voids or abnormal enhancing vessels and their location (central, peripheral or both), degree of contrast enhancement as minimal (barely visible), moderate (visible but < vessels) or intense (≥ vessels), and pattern of enhancement as homogenous (the entire tumor), heterogenous (only some areas enhanced) or peripheral (only the periphery enhanced). Tumor margins were assessed on post-contrast imaging or, when not available, on the sequence which best visualized them, and were categorized as predominantly (≥ 50%) sharp or poorly defined. Note was made when tumor contours were lobulated (lumpy, not smooth) and when internal tumor architecture appeared nodular (individual rounded structures). The presence of target-like lesions (small round lesions with central and peripheral signal or enhancement differences) was recorded. Tumor anatomic location and origin (arising from muscle, fat or indeterminate) were also recorded. When the split-fat sign (fat surrounding the poles of an intramuscular tumor) was present, tumor origin was considered indeterminate. When applicable, the same parameters were assessed on axial, sagittal and coronal CT images. All cases but one were reviewed at a Syngo Picture Archive and Communications workstation (Siemens, Erlanger, Germany) and the workstation tools (eg. window, level, magnification) were used at the reviewer's discretion. One case was available only as hard-copy film.

Results

Demographics and anatomic imaging tumor features

Among 25 enrolled subjects with ASPS, 3 were excluded due to unavailability of preoperative imaging. Pre-therapy imaging for the remaining 22 was obtained from 18 local institutions. MR imaging was available for 16, CT for 3, and both MR and CT for 3. The demographics and clinical features of these 22 subjects are shown in in Table 1. By imaging, maximum tumor diameters ranged from 20.0 cm for a retroperitoneal tumor to 2.3 cm for an orbital tumor (median maximum diameter, 5.9 cm). Fifteen tumors (15/22, 68%) measured ≥ 5 cm in greatest dimension. Tumor volumes ranged from 869 mL for a thigh tumor to 2.9 mL for a hand tumor (median volume, 43.2 mL). Seventeen tumors arose from muscle; 5 were of indeterminate origin (centered in muscle but had a split-fat sign; Figs. 2C, 4A). Seven tumors (7/22, 32%) abutted the NV bundle and one paraspinal tumor invaded a neural foramen and the spinal canal (1/22, 5%). Six tumors (6/22, 27%) abutted bone and 3 (3/22, 14%) destroyed bone, 1 of which resulted in pathologic fracture (Fig. 1A). Six tumors (6/22, 27%) showed evidence of central necrosis. The MR and CT features of these tumors are described in detail below.

MRI Features

The 19 tumors imaged with MRI were in the following sites; thigh (n =8), chest-wall (n=2), upper arm (n = 2), calf (n = 2), and foot, forearm, hand, orbit and paraspinal area (n = 1 each). Eighteen of the 19 MRI examinations included pre-contrast imaging (T1W, n = 18; T2W, n = 18; STIR, n = 14) and 13 had post-contrast imaging (one subject had only post-contrast imaging). MRI signal characteristics and enhancement patterns are summarized in Table 2. Of these 19 tumors all had flow voids that were both central and peripheral in 18 (18/19, 95%; Fig 2A) and only peripheral in one (1/19, 5%). Sixteen tumors (16/19, 84%)

had large vessels emanating from the superior and inferior poles that converged toward the center of the tumor (Fig 2A). Fourteen of 18 (14/18, 78%) tumors imaged with a pre-contrast T1W sequence appeared slightly hyperintense to muscle (Figs 2B, 5A). Eighteen tumors (18/19, 95%) had predominantly sharp margins, although 12 (12/18, 67%) of these had poorly defined margins at the superior and inferior poles where large vessels were present (Fig 3). One paraspinal tumor infiltrated a neural foramen, one orbital tumor had poorly defined margins, and one foot tumor infiltrated between the bones of the foot. Therefore, 15 tumors (15/19, 79%) had at least partially poorly defined margins. Sixteen tumors (16/19, 84%) had lobulated contours (Figs. 4, 5B), and 16 also had a nodular internal architecture, with nodules that were separated by thin hypodense bands on T1W, T2W, or STIR images (Fig 2B, 4, 5B). The degree of enhancement was intense in 9 (9/13, 69%; Fig. 5C) and moderate in 4 (4/13, 31%; Fig 2C). Of four tumors with peripheral enhancement, all showed a thick peripheral enhancing rim surrounding central low signal intensity consistent with central necrosis (Fig. 6A). Fourteen (14/19, 74%) tumors had target lesions that were peripherally bright and centrally dark on T2W images (Figs 4 and 5B).

CT features

Six tumors were imaged with contrast-enhanced CT; two chest wall/breast tumors, and one each, pelvis, abdominal wall, thigh and a thoracic paraspinal muscle tumor. All six had prominent vessels located at the superior and inferior poles of the tumor. In one case, large tumor vessels were thrombosed (Fig 7A,B). Four tumors had predominantly sharp margins, however, two of these had infiltrative margins in the area of vessels. Two tumors had predominantly infiltrative margins. Therefore, 4 (4/6, 67%) had at least partially infiltrative margins. Five tumors had lobulated margins, all 6 had nodular internal architecture and all 6 had small rim enhancing target lesions (Fig 1B). All 6 tumors enhanced, five (5/6, 83%) showing intense enhancement and one, moderate. Three tumors showed evidence of central necrosis on CT (one of which was also imaged with MRI and had MR evidence of central necrosis). Two of these had a thick peripheral rim of enhancement and no central enhancement (Fig. 6B). The third, a very large thigh mass, had a very nodular thick enhancing peripheral rim involving the majority of the tumor and imperceptible tumor margins elsewhere (Fig. 1A). The combined MRI and CT features of all tumors are summarized in Table 3.

Pathological Review

The gross tumor specimens were not available for pathology review. Therefore, to assess the gross appearance of ASPS we reviewed pathology reports which were available for 15 excised tumors. The remaining 7 tumors underwent delayed resection after neo-adjuvant therapy (these tumors were diagnosed by inisional or needle biopsy). Of the 15 gross tumor specimens all were described as circumscribed, firm, fleshy, nodular masses ranging in size from 0.5 cm – 7.0 cm (mean 3.4 cm). Vascular invasion was evaluated in 10 specimens and was present in 9 (9/10, 90%). Prominent vascularity was commented on in two reports. One report noted that the tumor was being supplied by a “bleeder”. Comments regarding tumor hemorrhage were made in 6 reports and was present in 3 of these tumors. These 3 did not have evidence of hemorrhage by imaging (all imaged with MRI only). Presence or absence

of necrosis was commented on in 4 reports, and central necrosis was documented in 1. This tumor showed evidence of necrosis on both MRI and CT.

Discussion

Due to the rarity of ASPS, only case reports and small case series describing the imaging features of this tumor are available in the literature. The COG ARST0332 multi-institutional trial for treatment of non-rhabdomyosarcoma soft-tissue sarcomas gave us the opportunity to more comprehensively assess the imaging features of this rare tumor in a relatively large cohort of young patients. When the clinicopathological features of ASPS were initially described in 1952, Christopherson and colleagues noted that “the most striking feature of the alveolar soft-part sarcoma is the basic uniformity throughout a given tumor and the similarity of one tumor to another” [9]. We also found that, by imaging, these tumors appear strikingly similar to one another and have unique imaging features that should suggest their diagnosis.

The most consistent imaging feature of ASPS in our study was the presence of intra and peri-tumoral vessels. All 19 tumors imaged with MRI had flow voids, consistent with high flow vessels; in 18 (18/19, 95%) flow voids were present at both the periphery and center of the tumor. This MR finding has been reported to be a feature of this tumor and, as in our study, has been described to be present at both the periphery and center of the tumor [12-17]. The majority of our tumors (19/22, 86%) also had large vessels at the superior and inferior poles that were evident by MRI and CT and, similar to the recent report by Viry and colleagues, seemed to converge toward the center of the tumor [12]. These features are also consistent with others who reported the highly vascular nature of ASPS on imaging studies [8, 12-14, 16-18]. Several investigators who reported the conventional angiographic findings of ASPS all describe similar findings on angiography. This hypervascular tumor demonstrates numerous enlarged vessels with arteriovenous shunting in the arterial phase followed by intense tumor staining. In spite of the rapid shunting of blood, washout of the contrast material from the lesion is slow [14-17]. This somewhat stagnant venous drainage may partially explain the presence of thrombosed tumor vessels in the case of a very large pelvic tumor in our series. Alternatively, these thrombi could have been due to direct vascular invasion by tumor, which was a common pathological feature (9/10, 90%) of tumors in our series. In contrast to others who have reported intense enhancement of all ASPS on MRI or CT, we found that 31% of tumors demonstrated only moderate enhancement [8, 12, 15-16]. Importantly, no tumor in our study showed minimal enhancement or a complete lack of enhancement. This difference between our results and others could be due to our larger sample size and the subjective nature of assessing the degree of contrast enhancement on imaging studies.

Consistent with prior reports we found that ASPS is either isointense or, more commonly, slightly hyperintense to muscle on MR T1W images [8, 12, 15-16]. This unique feature is in contrast to the majority of pediatric soft tissue sarcomas which appear hypointense on T1W images [19]. The etiology of this finding is unclear but has been postulated to be due either to the effect of chemotherapy or slow capillary blood flow within the tumor [12, 15-16]. Because all tumors in our study were imaged prior to initiation of treatment chemotherapy,

this can be excluded as a cause of this finding in our cohort. Other tumors that may appear hyperintense on T1W MRI include hemangioma, clear cell sarcoma, melanoma and hemorrhagic soft tissue tumors including the most common soft-tissue sarcoma in children, rhabdomyosarcoma. Clear cell sarcoma and melanoma appear hyperintense on T1W images when melanocytic differentiation is present. However, unlike ASPS, these tumors lack flow voids. The fibrofatty component of hemangiomas may appear hyperintense on T1W images and this tumor may contain flow voids. However, hemangiomas lack the large tumor vessels typical of ASPS, do not become centrally necrotic (as we found in 27% of our cases), and occur in a younger age group [20]. While hemorrhage in other soft-tissue tumors such as rhabdomyosarcoma, may appear hyperintense on T1W images (depending on the age of blood products) the non-hemorrhagic, solid component of most pediatric soft tissue malignancies will remain hypointense on this MR sequence in contrast to ASPS which is typically slightly hyperintense [19]. It is interesting to note that 3 tumors in our series showed pathological evidence of hemorrhage that was not present on MRI. It is possible that the hemorrhage in these tumors occurred after the imaging was obtained although we are unable to validate this.

We identified several additional imaging features that have not been previously reported for ASPS. Intra and peri-tumoral target lesions, that were small, peripherally bright and centrally dark on T2W MR images or, on CT showed a rim of peripheral enhancement, were a common finding in our study and consistent with the presence of numerous small tumor vessels. The target sign has been described as being nearly pathognomonic of peripheral nerve sheath tumors (PNST) and is attributed to central fibrosis and collagen resulting in low T2 signal intensity, and myxoid tissue peripherally producing high signal [21-23]. However, target lesions associated with PNSTs tend to be larger and more variable in size in contrast to the targets lesions seen in our study which were small and uniform. Additionally neurogenic tumors lack prominent vessels that are seen with ASPS, a feature which should be useful in differentiating these two tumors. The majority of tumors in our study had lobulated margins (86%) and a nodular internal architecture (86%). Tumor nodules were separated by thin dark bands of tissue on water sensitive MR sequences. These bands might represent the fibrovascular septa seen on histopathological inspection that separate the pseudoalveolar or organoid arrangement of tumor cells [9, 24]. We also found that most tumors had sharply defined margins except at the poles where large tumor vessels were present. We speculate that this finding may be a reflection of peritumoral edema or direct tumor spread. Interestingly, all 15 tumors that underwent gross pathological inspection in our study were described as nodular and circumscribed. We also found that, when present, necrosis was always central in location and surrounded by a thick rim of enhancing, viable tumor. Because tumor vessels seem to course toward the center of tumors, we speculate that the highly vascularized central core becomes necrotic due to tumor vascular invasion that begins centrally and progresses to the periphery. Alternatively, this appearance could be due to stagnant blood flow or central hypoxia as the tumor outgrows its vascular supply. In the future, prospective studies that directly correlate the imaging and anatomical and microscopic pathological features of ASPS will allow a better understanding of the imaging features of this unique tumor.

The histogenic origin of ASPS remains uncertain although a myogenic or neural crest origin have been suggested [8]. Although analysis of histochemical markers support a myogenic theory [25], a study of the immunocytochemistry and biochemistry of 12 ASPS found that none were positive for myoglobin or muscle actin and none expressed nuclear MyoD1 or myogenin [26]. While the majority of tumors in our study appeared to arise from muscle, 5 exhibited the split-fat sign which is known to be associated with neurogenic tumors that arise between muscles [21, 27]. Although ASPS is typically described as a well-circumscribed tumor, several in our study infiltrated adjacent structures; a neural foramen in one case and extension between metatarsals in another. An additional three tumors directly invaded bone, a finding that has been reported by others and illustrates the highly aggressive nature of this tumor [15, 17].

Our study has several limitations. Because imaging was obtained at 18 different institutions there was some variability in image quality and in the MR sequences that were obtained. However, all images were of sufficient quality to allow accurate assessment of the imaging features of the tumors. Although our sample size is relatively large given the rarity of this tumor, is does remain moderate at best. Also, for practical reasons, the ARST0332 protocol did not require central review of gross pathology specimens. Therefore, our assessment of the anatomic pathological features of the tumors was based on the pathology reports rather than a central review of pathological specimens. As such, we were unable to directly correlate imaging features with pathological findings for many of our tumors.

In conclusion, despite the rarity of ASPS we have reviewed the MR and CT imaging features of a relatively large cohort. This has allowed us to perform a more comprehensive assessment of the imaging features of this tumor than has been possible previously. Our findings are in agreement with others who have described the extremely vascular nature of this tumor. A diagnosis of ASPS should be considered when a solid tumor arising in muscle is slightly hyperintense to muscle on pre-contrast T1W MR images, contains flow-voids, has large vessels at the poles and demonstrates moderate to intense contrast enhancement. Additional features that we identified, and have not been previously reported, are the presence of small target lesions and a nodular internal architecture. Tumor margins tend to be lobulated and sharply defined, except in areas where vessels are present. When necrosis is present it is located centrally and surrounded by a thick rim of enhancing solid tumor. In the future, a direct correlation between the imaging features and the anatomic pathological findings will further our understanding of the imaging appearance of this rare and unique tumor.

Acknowledgements

The authors thanks Anne Speights, Edwina Anderson and Ellen Tsan for their assistance in data collection and management and Fran Laurie for her assistance with imaging processing and transfer from QARC.

Supported by CA98543, U10 CA98413

References

1. Primrose, JN. Soft Tissue Tumours. 3rd ed.. Enzinger, FM.; Weiss, SW., editors. Mosby-Year-Book; St. Louis, MO: 1995. p. 1120

2. Pennacchioli E, Fiore M, Collini P, et al. Alveolar soft part sarcoma: clinical presentation, treatment, and outcome in a series of 33 patients at a single institution. Ann Surg Oncol. 2010:3229–3233. [PubMed: 20593242]

3. Pizzo, PA.; Poplack, DG. Principles and Practice of Pediatric Oncology. 6th ed.. Williams&Wilkins; Philadelphia, PA: 2011. p. 971-972.

4. Orbach D, Brennan B, Casanova M, et al. Paediatric and Adolescent Alveolar Soft Part Sarcoma: A Joint Series from European Cooperative Groups. Pediatr Blood Cancer. 2013:1826–1832. [PubMed: 23857870]

5. Lieberman PH, Brennan MF, Kimmel M, Erlandson RA, Garin-Chesa P, Flehinger BY. Alveolar soft-part sarcoma. A clinico-pathologic study of half a century. Cancer. 1989:1–13. [PubMed: 2642727]

6. Casanova M, Ferrari A, Bisogno G, et al. Alveolar soft part sarcoma in children and adolescents: A report from the Soft-Tissue Sarcoma Italian Cooperative Group. Ann Oncol. 2000:1445–1449. [PubMed: 11142485]

7. Koguchi Y, Yamaguchi T, Yamato M, Osada D, Saotome K. Alveolar soft part sarcoma of bone. J Orthop Sci. 2005:652–655. [PubMed: 16307193]

8. Kim HS, Lee HK, Weon YC, Kim HJ. Alveolar soft-part sarcoma of the head and neck: clinical and imaging features in five cases. AJNR Am J Neuroradiol. 2005:1331–1335. [PubMed: 15956492]

9. Christopherson WM, Foote FW Jr. Stewart FW. Alveolar soft-part sarcomas; structurally characteristic tumors of uncertain histogenesis. Cancer. 1952:100–111. [PubMed: 14886902]

10. Folpe AL, Deyrup AT. Alveolar soft-part sarcoma: a review and update. J Clin Pathol. 2006:1127–1132. [PubMed: 17071801]

11. Williamson SR, Bunde PJ, Montironi R, et al. Malignant perivascular epithelioid cell neoplasm (PEComa) of the urinary bladder with TFE3 gene rearrangement: clinicopathologic, immunohistochemical, and molecular features. Am J Surg Pathol. 2013:1619–1626. [PubMed: 23797724]

12. Viry F, Orbach D, Klijanienko J, et al. Alveolar soft part sarcoma-radiologic patterns in children and adolescents. Pediatr Radiol. 2013:1174–1181. [PubMed: 23681452]

13. Daly BD, Cheung H, Gaines PA, Bradley MJ, Metreweli C. Imaging of alveolar soft part sarcoma. Clin.Radiol. 1992:253–256. [PubMed: 1424447]

14. Aiken AH, Stone JA. Alveolar soft-part sarcoma of the tongue. AJNR Am J Neuroradiol. 2003:1156–1158. [PubMed: 12812945]

15. Suh JS, Cho J, Lee SH, et al. Alveolar soft part sarcoma: MR and angiographic findings. Skeletal Radiol. 2000:680–689. [PubMed: 11271548]

16. Iwamoto Y, Morimoto N, Chuman H, Shinohara N, Sugioka Y. The role of MR imaging in the diagnosis of alveolar soft part sarcoma: a report of 10 cases. Skeletal Radiol. 1995:267–270. [PubMed: 7644939]

17. Lorigan JG, O'Keeffe FN, Evans HL, Wallace S. The radiologic manifestations of alveolar soft-part sarcoma. AJR Am J Roentgenol. 1989:335–339. [PubMed: 2750619]

18. Pang LM, Roebuck DJ, Griffith JF, Kumta SM, Metreweli C. Alveolar soft-part sarcoma: a rare soft-tissue malignancy with distinctive clinical and radiological features. Pediatr Radiol. 2001:196–199. [PubMed: 11297086]

19. Stein-Wexler R. Pediatric soft tissue sarcomas. Semin Ultrasound CT MR. 2011:470–488. [PubMed: 21963167]

20. Dubois J, Garel L. Imaging and therapeutic approach of hemangiomas and vascular malformations in the pediatric age group. Pediatr Radiol. 1999:879–893. [PubMed: 10602864]

21. Murphey MD, Smith WS, Smith SE, Kransdorf MJ, Temple HT. From the archives of the AFIP. Imaging of musculoskeletal neurogenic tumors: radiologic-pathologic correlation. Radiographics. 1999:1253–1280. [PubMed: 10489179]

22. Suh JS, Abenoza P, Galloway HR, Everson LI, Griffiths HJ. Peripheral (extracranial) nerve tumors: correlation of MR imaging and histologic findings. Radiology. 1992:341–346. [PubMed: 1561333]

23. Burk, Jr DL.; Brunberg, JA.; Kanal, E.; Latchaw, RE.; Wolf, GL. Spinal and paraspinal neurofibromatosis: surface coil MR imaging at 1.5 T1. Radiology. 1987:797–801. [PubMed: 3101136]

24. Daigeler A, Kuhnen C, Hauser J, et al. Alveolar soft part sarcoma: clinicopathological findings in a series of 11 cases. World J Surg Oncol. 2008:71. [PubMed: 18593459]

25. Sciot R, Dal Cin P, De Vos R, et al. Alveolar soft-part sarcoma: evidence for its myogenic origin and for the involvement of 17q25. Histopathology. 1993:439–444. [PubMed: 8314217]

26. Wang NP, Bacchi CE, Jiang JJ, McNutt MA, Gown AM. Does alveolar soft-part sarcoma exhibit skeletal muscle differentiation? An immunocytochemical and biochemical study of myogenic regulatory protein expression. Mod Pathol. 1996:496–506. [PubMed: 8733764]

27. Jee WH, Oh SN, McCauley T, et al. Extraaxial neurofibromas versus neurilemmomas: discrimination with MRI. AJR Am J Roentgenol. 2004:629–633. [PubMed: 15333347]

Figure 1.

19 yo male with alveolar soft part sarcoma (ASPS) of the thigh. A) Coronal reconstructed CT image shows the primary tumor (straight arrow) with bone invasion (curved arrow) and pathologic fracture. B) Sagittal reconstructed image shows rim enhancing target lesions (arrow). Stabilization hardware caused streak artifact in these images.

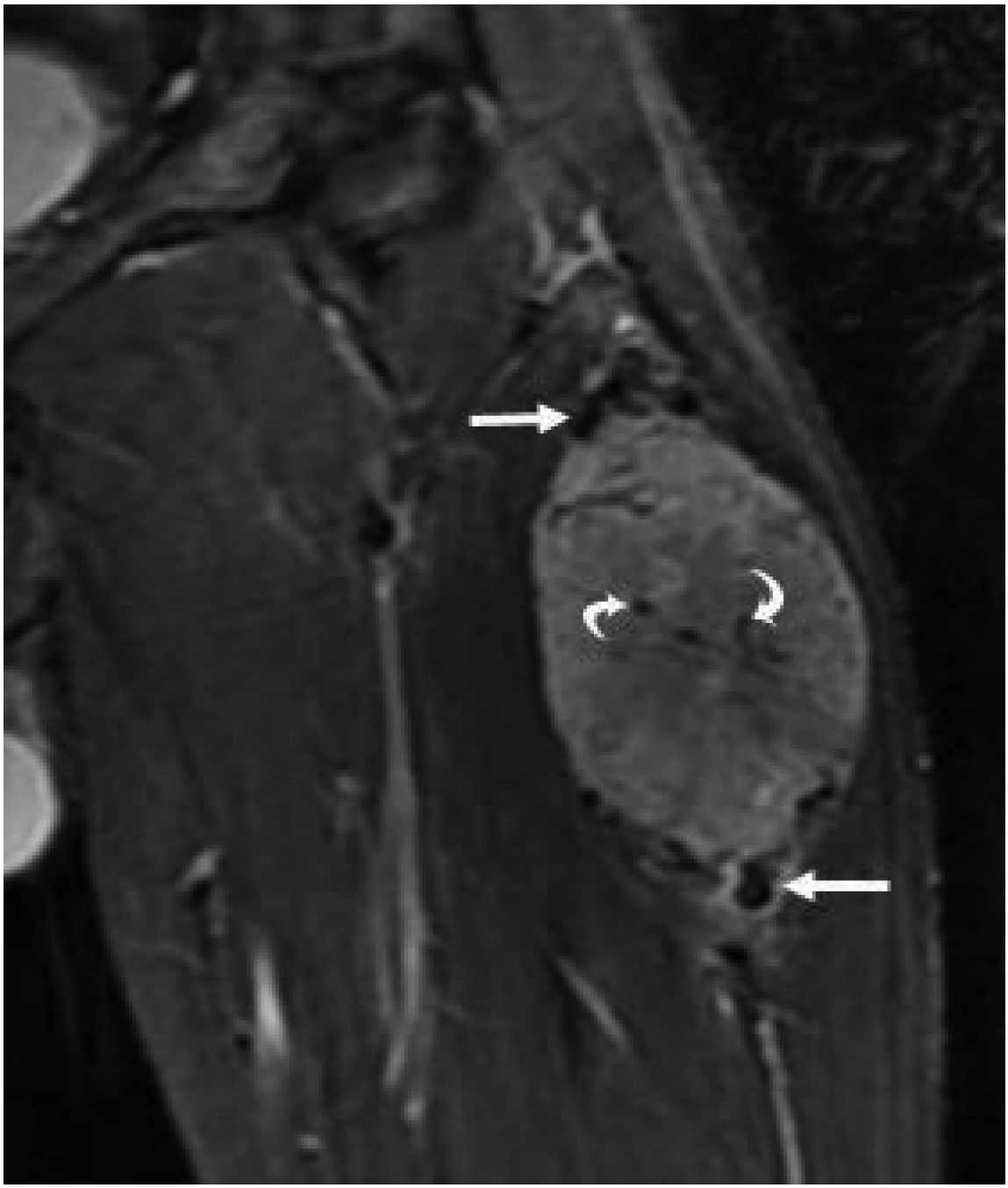

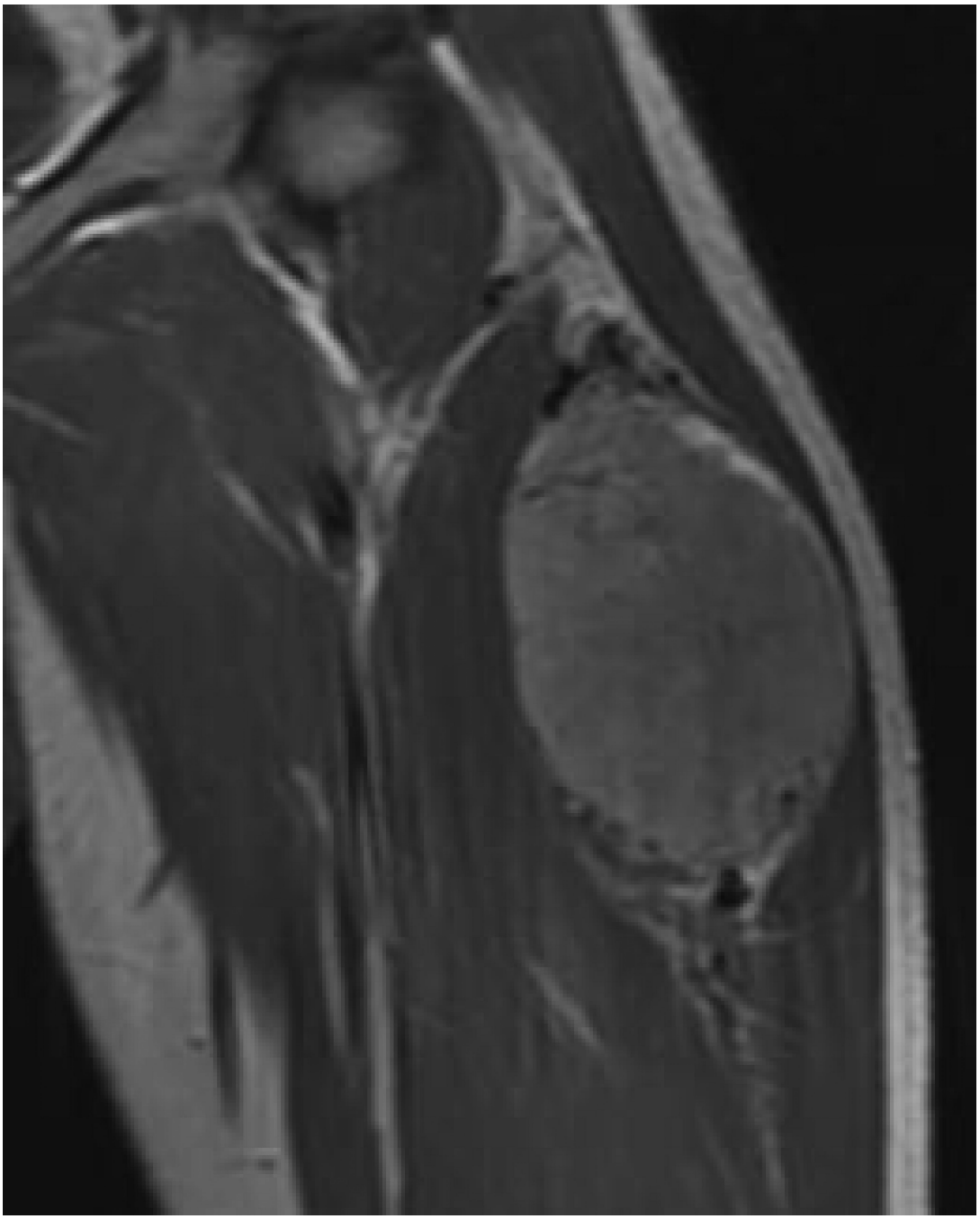

Figure 2.

21 yo male with ASPS of the thigh. A) Short tau inversion recovery (STIR; TR 3000ms/TE 52.5 ms) coronal MR image shows large vessels at superior and inferior poles (straight arrows) and central flow voids (curved arrows). B) Axial T1W (TR 516.6 ms/TE 13.0 ms) non-contrast enhanced MR image shows slightly hyperintense tumor (T). Note thin dark bands separating tumor nodules (a few indicated with arrows). C) Coronal T1W (TR 783.3 ms/TE 13.0 ms) post-contrast MR image shows moderate tumor enhancement. The split-fat sign is present at the poles.

Figure 3.
9 yo male with ASPS of the calf. This T1W (TR 666.7/TE 13.3) contrast-enhanced coronal MR image shows a sharply marginated tumor except at the superior and inferior poles where vessels are present (arrows).

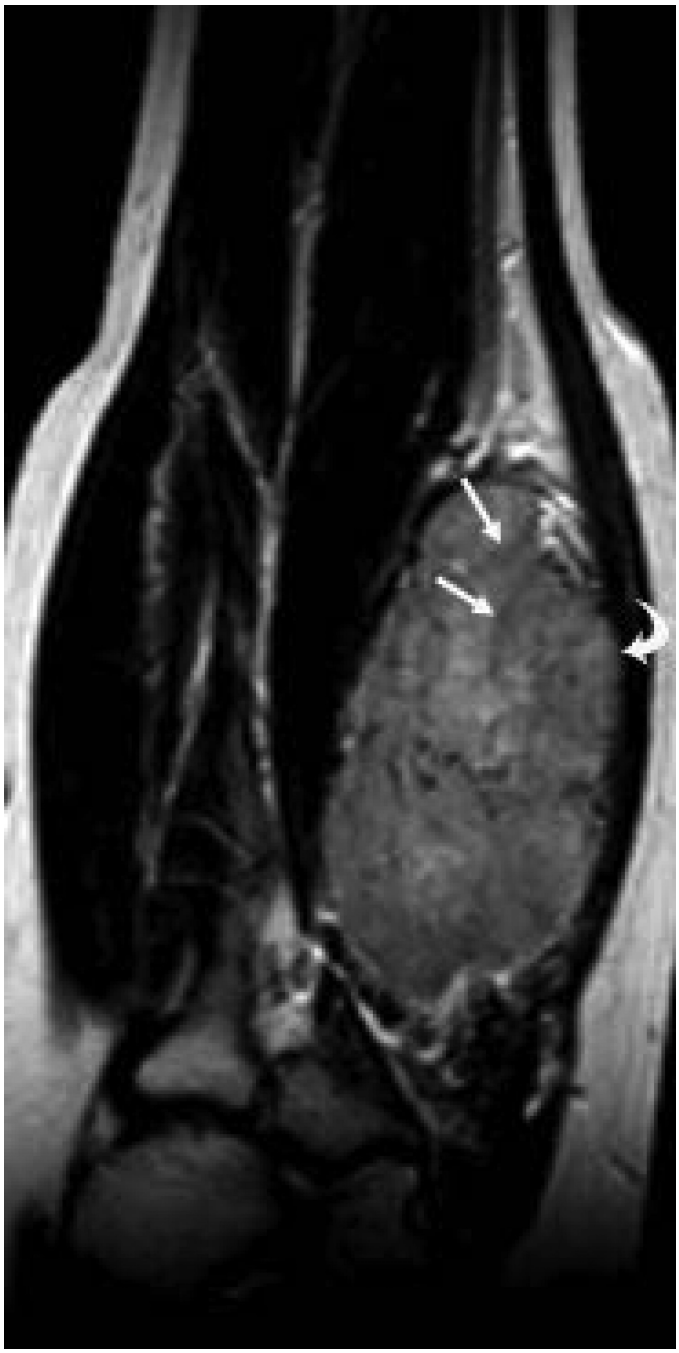

Figure 4.
17 yo female with ASPS of the calf. T2W (TR 5100 ms/TE 91.0 ms) non-fat supressed coronal image shows lobulated contour and thin hypointense bands (a few indicated with straight arrows) separating tumor nodules. Note small targets lesions with bright periphery and dark centers (curved arrow) and split-fat sign at the poles.

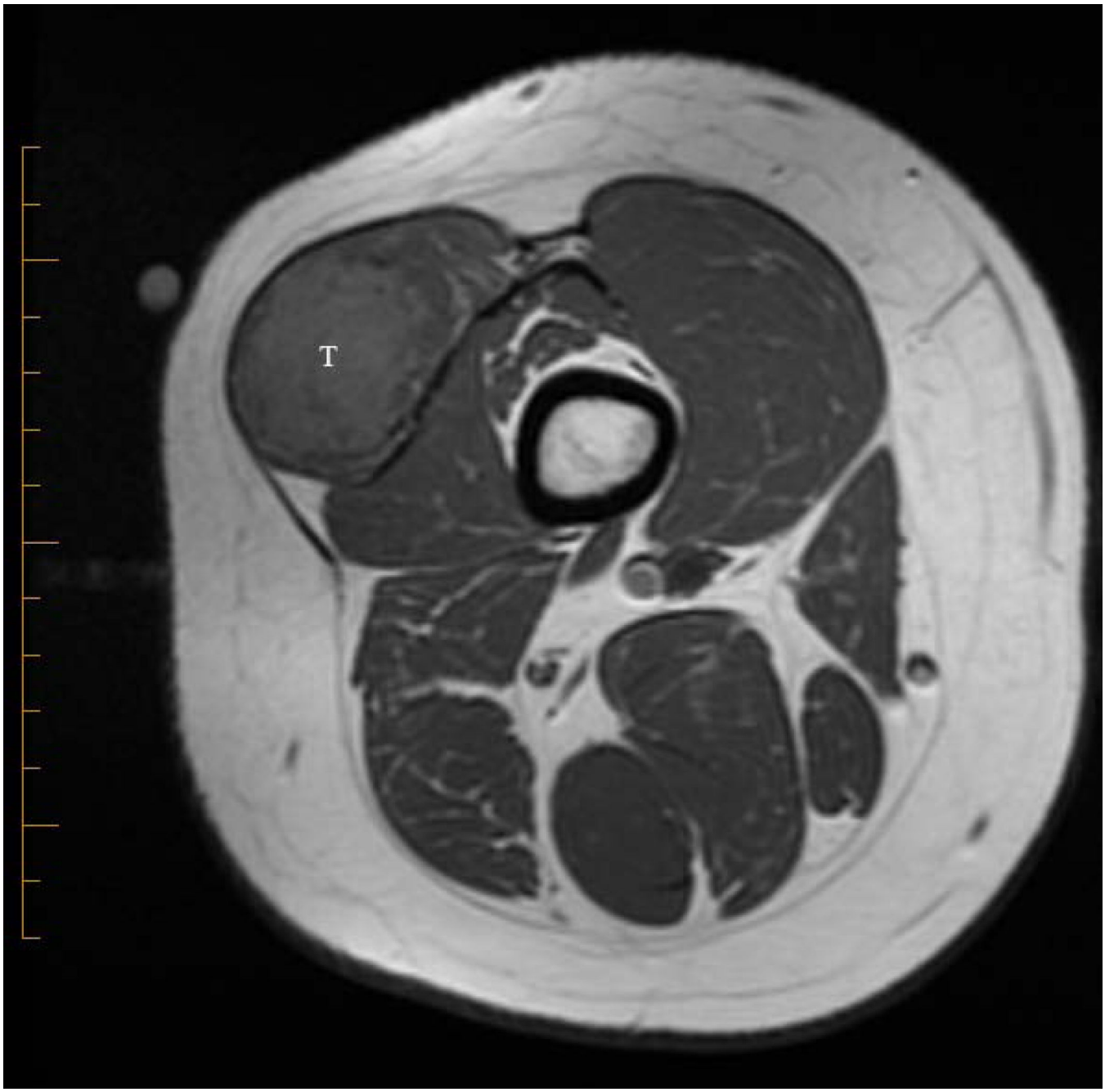

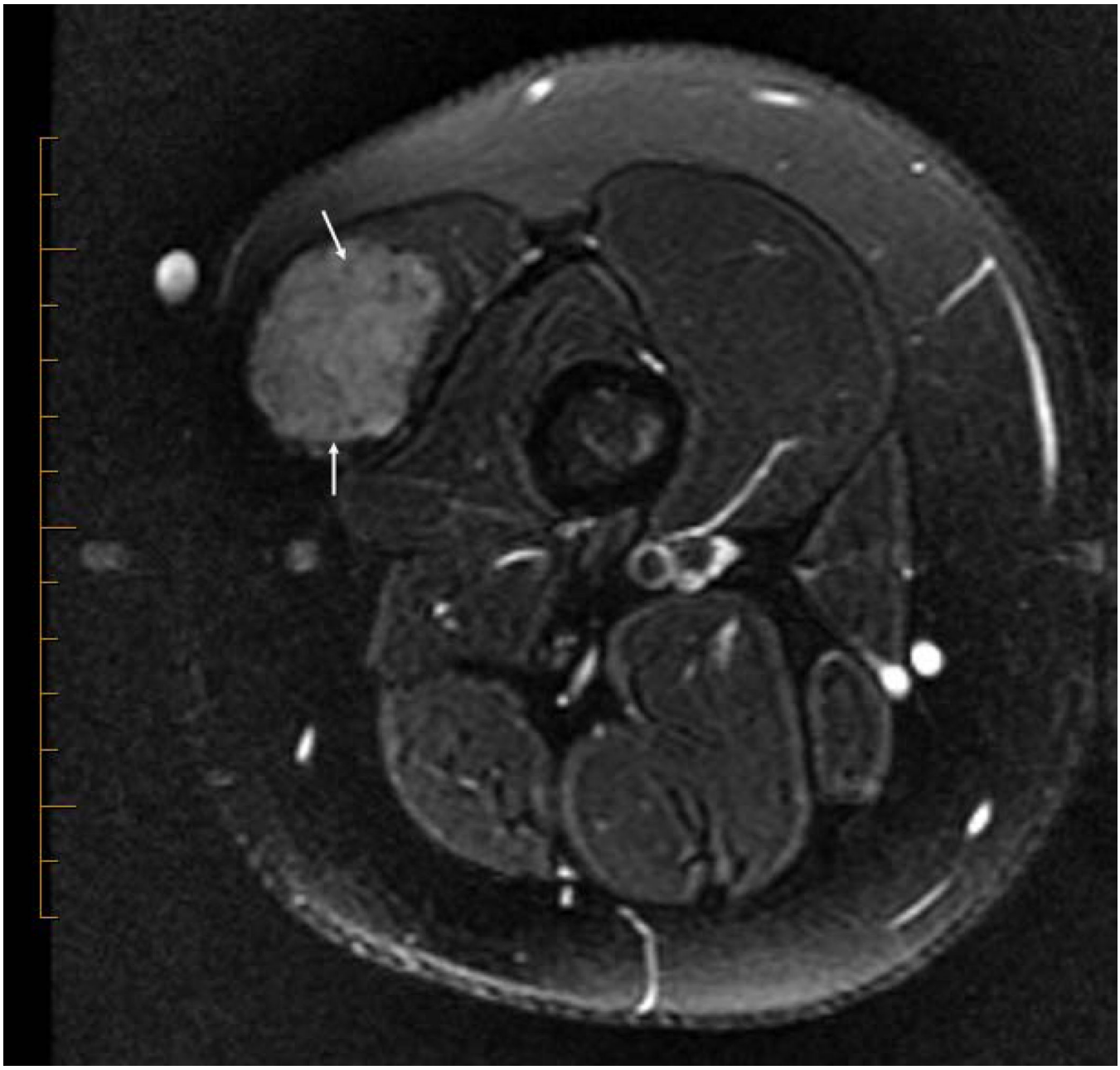

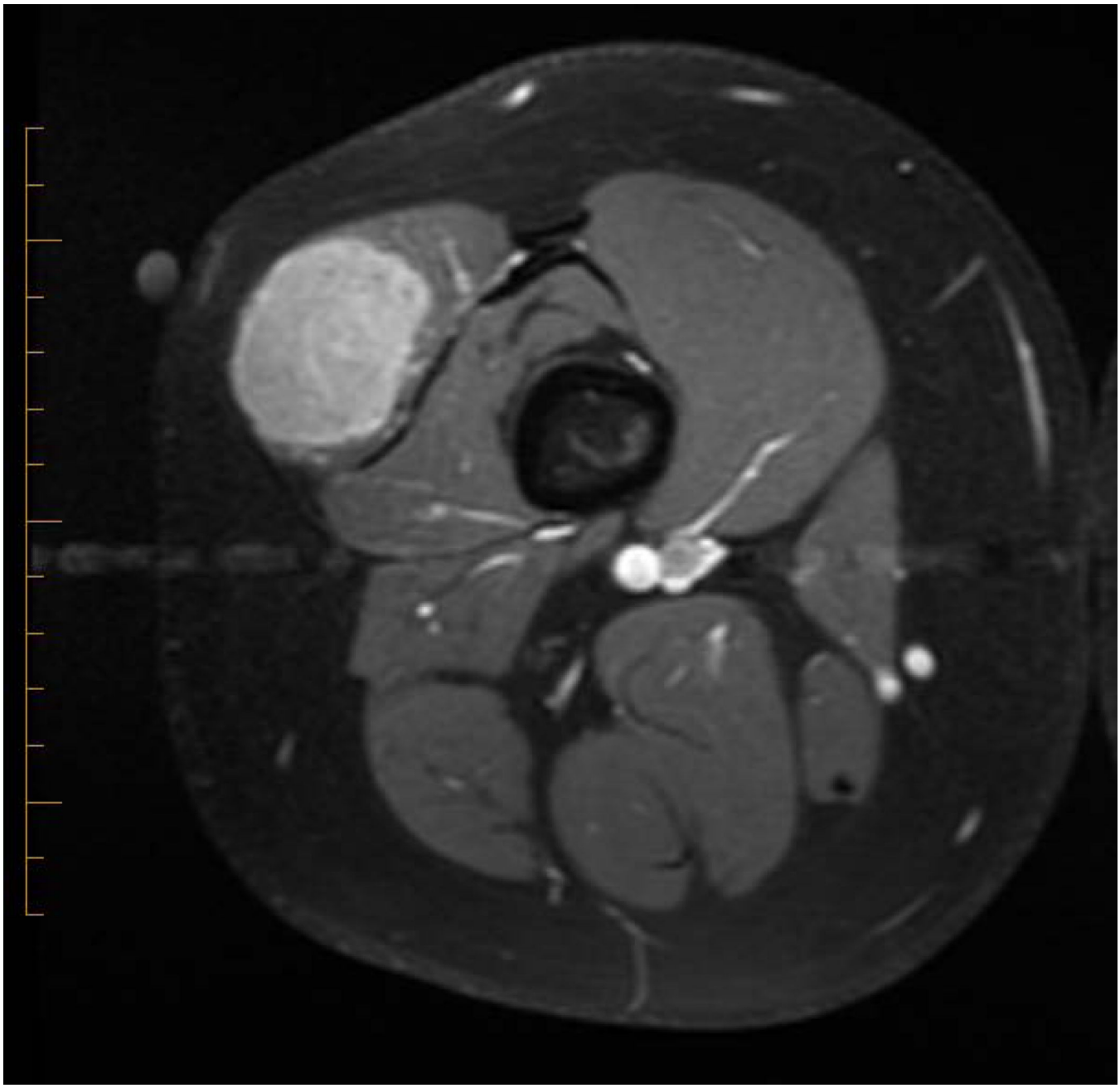

Figure 5.

14 yo female with ASPS of the thigh. A) T1W (TR 647.0 ms/TE 9.94 ms) non-contrast enhanced axial MR image shows slightly hyperintense tumor (T). B) T2W (TR 4050.0 ms/TE 96.2 ms) axial MR image shows tumor has lobulated contours and nodular internal architecture. Note small target lesions with bright periphery and dark centers (arrows). C) T1W (TR 550.0 ms/TE 9.98 ms) contrast-enhanced axial image shows intense tumor enhancement.

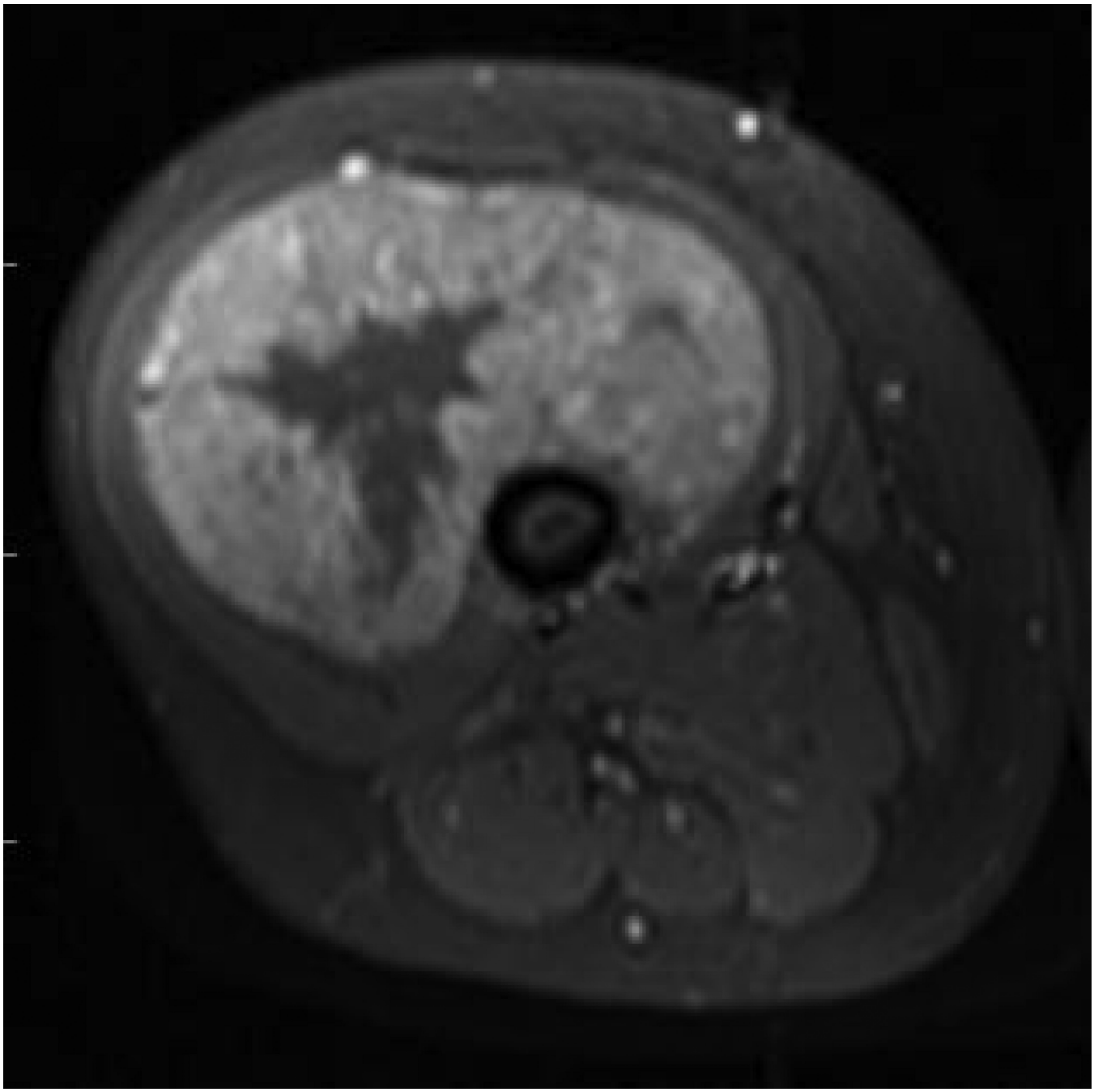

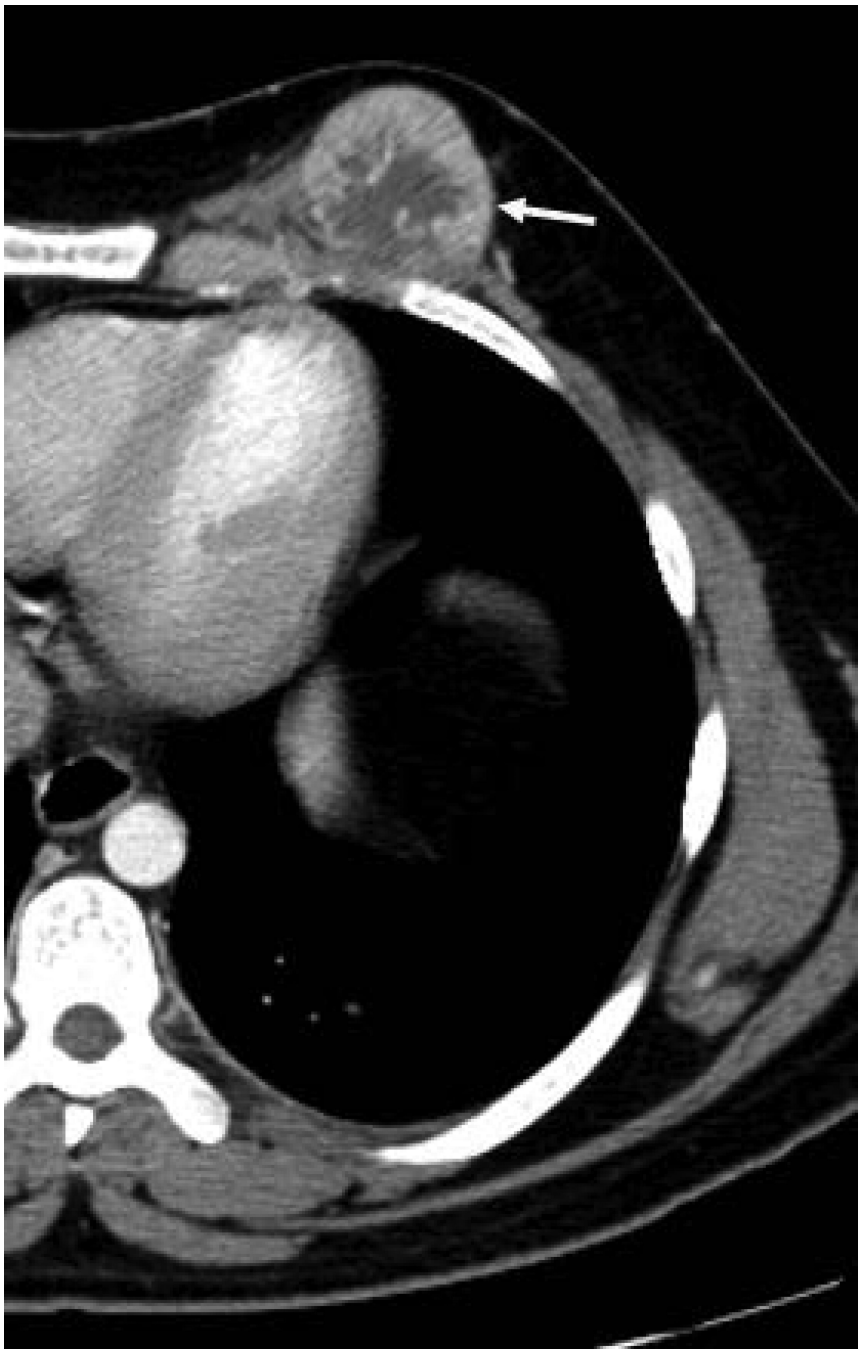

Figure 6.

A) 12 yo female with ASPS of the thigh, T1W (TR 700 ms/TE 14.0 ms) contrast-enhanced axial MR image and B) 17 yo female with breast ASPS, axial contrast enhanced CT image, both show thick enhancing peripheral rim and non-enhancing center consistent with central necrosis.

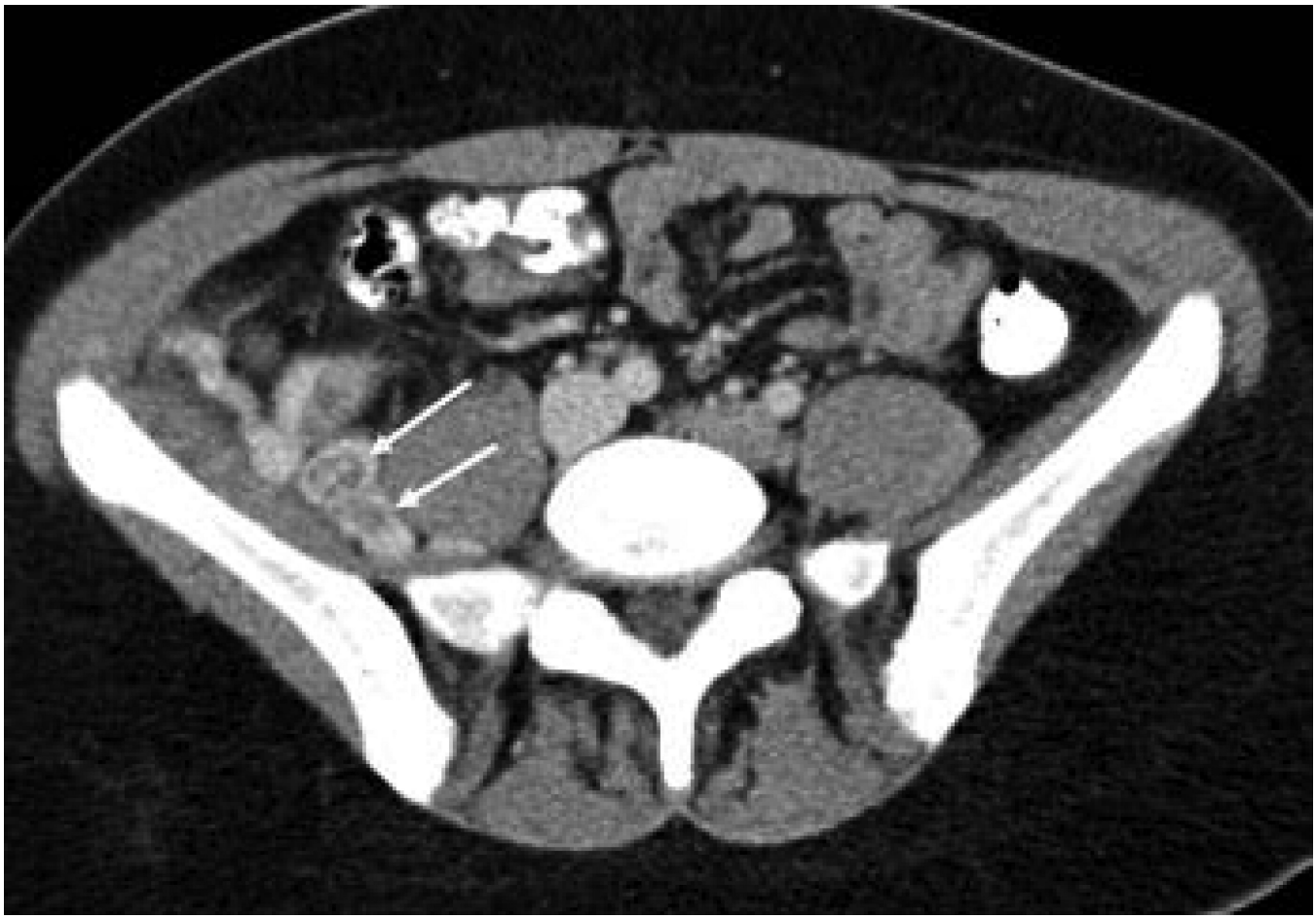

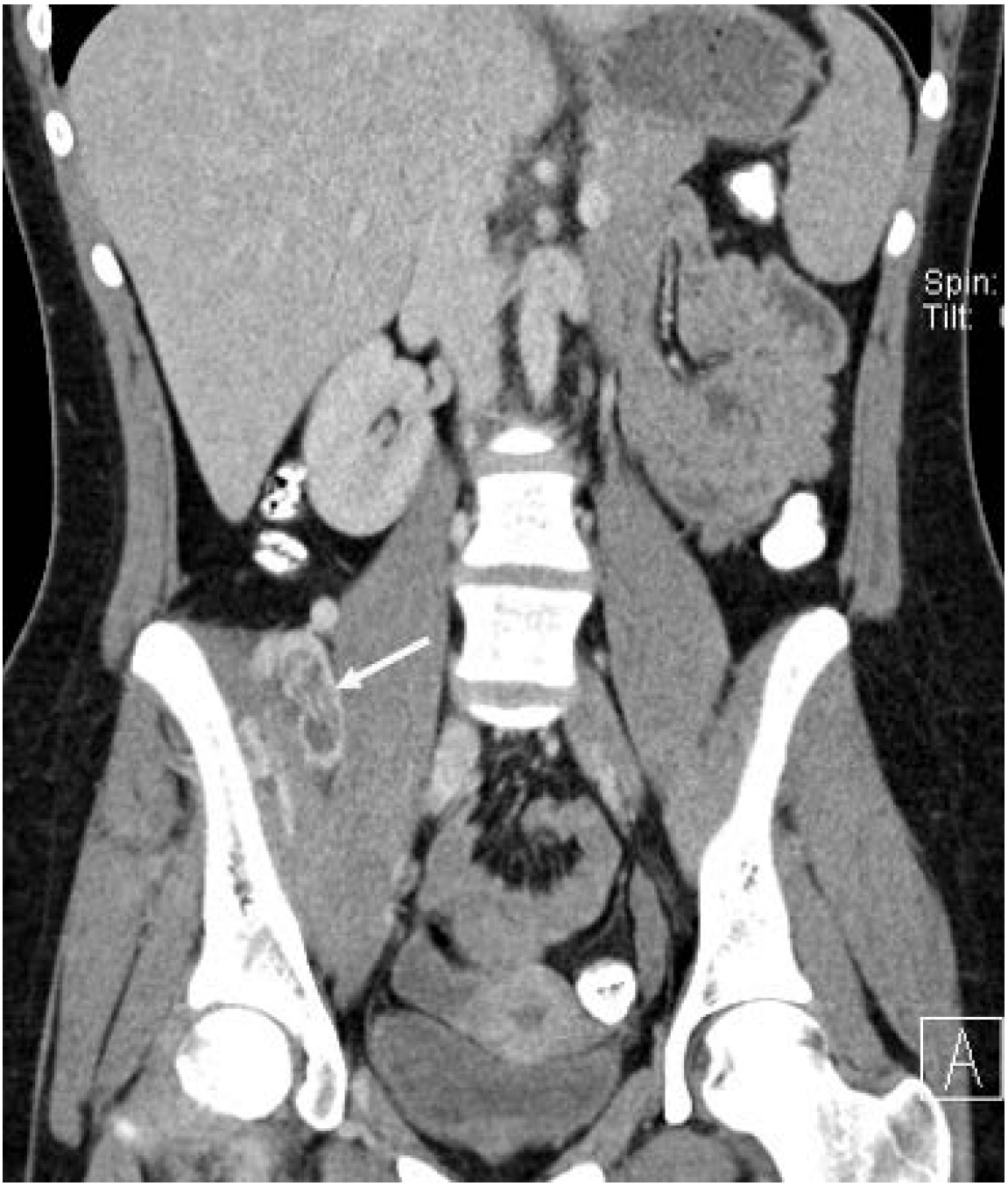

Figure 7.
17 yo female with pelvic ASPS. A) axial and B,C) coronal reconstructed contrast-enhanced CT images show large thrombosed vessels (arrows) at the periphery of C) the large primary tumor (T).

Table 1

Demographic and clinical features at diagnosis of alveolar soft part sarcoma in 22 subjects.

Age at diagnosis	**Mean 15.7 yrs, range, 8-23.6 yrs**
Characteristic	**N (%)**
Gender	
Female	12 (12/22, 54%)
Male	10 (10/22, 46%)
Primary Tumor Sites	
Lower extremity:	12 (12/22, 55%)
Thigh	9
Calf	2
Foot	1
Upper extremity	4 (4/22, 18%)
Upper arm	2
Forearm	1
Hand	1
Chest	3 (3/22, 14%)
Thoracic paraspinal	1
Breast/chest wall	2
Abdomen/pelvis: n = 2	2 (2/22, 9%)
Abdominal wall	1
Iliopsoas muscle	1
Orbit	1 (1/22, 5%)
Metastatic disease	11 (11/22, 50%)
Both lungs	8
Both lungs and bone	1
Both lungs, bone and liver	1
Both lungs and brain	1

Table 2

Magnetic resonance imaging features of 19 alveolar soft part sarcomas

Pre-Contrast				
	Hypointense N (%)	**Isointense N (%)**	**Hyperintense N (%)**	**Mixed N (%)**
T1W	0	3 (3/18, 17%)	*14 (14/18, 78%)	1 (1/18, 5%)
T2W	0	1 (1/17, 6%)	15 (15/17, 88%)	1 (1/17, 6%)
STIR	0	0	13 (13/14, 93%)	1 (1/14, 7%)
Post-Contrast				
	Degree of Enhancement N (%)			
Minimal	0			
Moderate	4 (4/13, 31%)			
Intense	9 (9/13, 69%)			
	Pattern of Enhancement N (%)			
Homogenous	9 (9/13, 69%)			
Peripheral	4 (4/13, 31%)			
Heterogenous	0			

* tumors slightly hyperintense to muscle

Table 3

[*] Combined MRI and CT Imaging features of 22 alveolar soft part sarcomas

Imaging Feature	N (%)
Flow voids (feature seen only on MR, total number MRs = 19)	19 (19/19, 100%)
Large vessels at poles	19 (19/22, 86%)
Lobulated contour	19 (19/22, 86%)
Nodular internal architecture	19 (19/22, 86%)
Target lesions	14 (14/22, 64%)
Degree of Enhancement (number of post contrast exams = 16)	
Minimal	0
Moderate	5 (5/16, 31%)
Intense	11 (11/16, 69%)
Central necrosis	6 (6/16, 38%)

[*] Data collected from 19 MRI and 3 CT examinations. For 3 subjects who had both MR and CT, only MR data is reported here.